Pharm Res (2012) 29:770–781
DOI 10.1007/s11095-011-0601-8

RESEARCH PAPER

Lapatinib Distribution in HER2 Overexpressing Experimental Brain Metastases of Breast Cancer

Kunal S. Taskar • Vinay Rudraraju • Rajendar K. Mittapalli • Ramakrishna Samala • Helen R. Thorsheim • Julie Lockman • Brunilde Gril • Emily Hua • Diane Palmieri • Joseph W. Polli • Stephen Castellino • Stephen D. Rubin • Paul R. Lockman • Patricia S. Steeg • Quentin R. Smith

Received: 31 July 2011 / Accepted: 21 September 2011 / Published online: 20 October 2011

ABSTRACT

Purpose Lapatinib, a small molecule EGFR/HER2 inhibitor, partially inhibits the outgrowth of HER2+ brain metastases in preclinical models and in a subset of CNS lesions in clinical trials of HER2+ breast cancer. We investigated the ability of lapatinib to reach therapeutic concentrations in the CNS following ^{14}C-lapatinib administration (100 mg/kg *p.o.* or 10 mg/kg, *i.v.*) to mice with MDA-MD-231-BR-HER2 brain metastases of breast cancer.

Methods Drug concentrations were determined at differing times after administration by quantitative autoradiography and chromatography.

Results ^{14}C-Lapatinib concentration varied among brain metastases and correlated with altered blood-tumor barrier permeability. On average, brain metastasis concentration was 7–9-fold greater than surrounding brain tissue at 2 and 12 h after oral administration. However, average lapatinib concentration in brain metastases was still only 10–20% of those in peripheral metastases. Only in a subset of brain lesions (17%) did lapatinib concentration approach that of systemic metastases. No evidence was found of lapatinib resistance in tumor cells cultured *ex vivo* from treated brains.

Conclusions Results show that lapatinib distribution to brain metastases of breast cancer is partially restricted and blood-tumor barrier permeability is a key component of lapatinib therapeutic efficacy which varies between tumors.

KEY WORDS brain metastases · breast cancer · epidermal growth factor receptors · lapatinib · HER2

ABBREVIATIONS

BBB	blood–brain barrier
BCRP	breast cancer resistance protein
BTB	blood-tumor barrier
CNS	central nervous system
EGFP	enhanced green fluorescent protein
EGFR	epidermal growth factor receptor
MRP	multidrug resistance protein
P-gp	p-glycoprotein

INTRODUCTION

Breast cancers frequently overexpress members of the epidermal growth factor receptor (EGFR) family, such as EGFR and HER2, which are linked to intracellular tyrosine kinase signaling pathways that promote tumor cell proliferation, invasion, metastasis, angiogenesis and resistance to therapy (1). HER2 is amplified in 25–30% of human breast cancers and is associated with enhanced

K. S. Taskar · V. Rudraraju · R. K. Mittapalli · R. Samala · H. R. Thorsheim · P. R. Lockman · Q. R. Smith (✉)
Department of Pharmaceutical Sciences
Texas Tech University Health Sciences Center
1406 Coulter Drive
Amarillo, Texas 79106, USA
e-mail: Quentin.Smith@ttuhsc.edu

J. Lockman
Department of Biological Sciences
West Texas A&M University
Canyon, Texas 79016, USA

B. Gril · E. Hua · D. Palmieri · P. S. Steeg
Women's Cancers Section, Laboratory of Molecular Pharmacology
National Cancer Institute, National Institutes of Health
Bethesda, Maryland 20892, USA

J. W. Polli · S. Castellino
GlaxoSmithKline
Research Triangle Park, North Carolina 27709, USA

S. D. Rubin
GlaxoSmithKline
Collegeville, Pennsylvania 19426, USA

tumor aggressiveness and reduced patient survival (1,2). Despite advances in the systemic therapy for patients with HER2+ tumors, central nervous system (CNS, or brain) metastases remain a significant problem. More than one third of metastatic patients with HER2+ tumors develop brain metastases (3), many of which occur when the patient is responding to therapy or has stable systemic disease (4,5). Therapeutic options for the treatment of HER2+ brain metastases of breast cancer are limited.

Trastuzumab, a humanized monoclonal antibody to HER2, is approved for the treatment of HER2+ breast cancer and shows efficacy against systemic tumors in combination with cytotoxic chemotherapy in the metastatic and adjuvant settings (6–8). However, a number of studies have reported increased rates of HER2+ CNS metastases in patients treated with trastuzumab therapy (4,5,9,10). Further, trastuzumab, as a large protein (MW = 145,000 Daltons), crosses the blood–brain barrier (BBB) poorly and reaches concentrations in CSF that are ~300 times lower than that in serum (11–13). Trastuzumab uptake is also limited in brain metastases, except at sites of marked barrier disruption (14–16). This has raised the concern that the brain may represent a sanctuary site in trastuzumab-treated patients allowing selective proliferation of HER2+ cancer cells.

The poor brain distribution of trastuzumab has stimulated interest in alternative anti-HER2 agents with improved BBB permeability. Lapatinib (Tykerb/Tyverb) is lipophilic, small drug inhibitor of HER2 and EGFR that has been approved for the treatment of HER2+ metastatic breast cancer that has progressed after prior taxanes, anthracyclines and trastuzumab therapy (17). Lapatinib acts by blocking the intracellular ATP-binding site of the tyrosine kinase domain, leading to reduced receptor phosphorylation and activation (18,19). Unlike trastuzumab, lapatinib can be administered orally and distributes well to many organs. But in normal brain, lapatinib uptake is <10% of plasma due to active efflux transport at the BBB (20,21). The BBB is partially compromised in brain metastases, resulting in a variably leaky blood-tumor barrier (BTB) (22,23). However, the ability of the BTB to limit lapatinib delivery in brain metastases has not been determined.

In clinical trials, lapatinib has shown partial efficacy for the treatment of brain metastases of HER2+ breast cancer. With monotherapy, the response rate is low, with only 6% of patients achieving an objective response and 21% experiencing a >20% reduction in lesion volume (24,25). However, combination therapy with capecitabine improved objective responses to 21%, with 48% of patients experiencing clinical benefit for >6 months (26,27). Lapatinib has also shown activity in the prevention of brain metastases in preclinical studies. Gril *et al.* (28) found that lapatinib reduced formation of large brain metastases in mice by 50–53% and decreased the extent of phosphorylated HER2 staining within HER2+ brain metastases when treatment was initiated early in the course of the disease. Long term follow-up of a Phase III lapatinib/capecitabine trial also showed a significant reduction in the number of brain metastases as a first site of relapse, consistent with the potential preventive effect of lapatinib (29). Thus, lapatinib may be of interest for both prevention and treatment of brain metastases of HER2+ breast cancer.

It remains unclear whether the limited efficacy of lapatinib against brain metastases is the result of inadequate drug delivery or due to development of drug-resistant cells within the nervous system that do not respond to treatment (25). No studies have evaluated lapatinib distribution to brain metastases in humans or in preclinical models. Using the MDA-MB-231-BR HER2 breast cancer cell line (231-BR-HER2) in immunocompromised mice, we recently showed that brain metastasis uptake of two cytotoxic chemotherapeutic drugs, paclitaxel and doxorubicin, though significantly elevated in most brain metastases relative to surrounding brain, was still 30-fold less that in peripheral metastases, indicative of a critical limiting role of the BTB. Consistent with this, cytotoxic effects were seen only in the small subset (10%) of brain metastases that displayed the highest drug concentrations. Therefore, for these two chemotherapeutic agents, the results suggested that BTB drug delivery critically limits therapeutic effect against brain metastases.

In this study we use the same 231-BR-HER2 model to investigate the extent to which ^{14}C-lapatinib is taken up into experimental brain metastases of breast cancer. Drug concentrations were determined in metastases in both brain and in systemic tissues (e.g., lung) using highly sensitive phosphorescence autoradiography (30) as well as HPLC/LC-MS/MS. The results show that brain metastasis uptake of ^{14}C-lapatinib is heterogeneous with concentrations in some brain metastases approaching 50% of those in peripheral lesions. However, in the great majority of brain metastases (>80%), lapatinib concentration was <10–20% of that in peripheral metastases. No evidence was found for lapatinib drug resistance in tumor cells isolated from lapatinib-treated brains, confirming the importance of inadequate drug uptake. The data suggest that variable and limited lapatinib exposure may contribute to brain metastatic progression.

MATERIALS AND METHODS

Materials

^{14}C-Lapatinib and unlabeled lapatinib (GW572016) were supplied by GlaxoSmithKline (GSK). Radiochemical purity

(>99%) was confirmed by reverse phase HPLC prior to administration. Texas Red dextran (3 kDa) was obtained from Invitrogen. The human MDA-MB-231-BR breast cancer cell line was kindly provided by Dr. Toshyaki Yoneda, University of Texas at San Antonio, San Antonio, TX. The MDA-MB-231-BR cells were transfected to express enhanced green fluorescent protein (EGFP) and to overexpress HER2 (28,31).

Brain Metastasis Model

All animal experiments were performed in accordance with the NIH Guide for the Care and Use of Animals following an approved IACUC protocol. Immunocompromised female NuNu mice (Charles River Laboratories, Frederick, MD) were anesthetized with isoflurane and inoculated into the left cardiac ventricle with 1.75×10^5 brain-seeking 231-BR-HER2 cells expressing EGFP (28,31). Metastases were allowed to develop for 4–6 weeks at which time animals began to exhibit neurological symptoms.

^{14}C-Lapatinib Distribution Kinetics and Autoradiography

^{14}C-Lapatinib (10.2 μCi/mg) was administered to animals (n=5–8 mice per time point) by oral gavage (100 mg/kg, 200 μL per mouse) or by single *i.v.* injection (10 mg/kg, 100 μL per mouse). In oral administration studies, lapatinib was formulated and delivered in a vehicle consisting of 0.5% hydroxypropylmethylcellulose with 0.1% Tween 80 in water (20,21). In *i.v.* injection studies, lapatinib was administered in DMSO diluted to 30% using 0.9% NaCl. Tracer was allowed to circulate for 2 or 12 h in the oral experiments and for 30 min in the i.v. experiments. Ten minutes prior to the end of the circulation period, animals were anesthetized with ketamine/xylazine and administered Texas Red 3 kDa dextran (Invitrogen; 1.5 mg/animal i.v.) for evaluation of BBB and BTB permeability. At the end of the circulation period, animals were euthanized and the brain as well as selected other tissues (e.g., liver, lung, heart, kidney) were rapidly removed (<30 s) and flash frozen in isopentane (−65°C). Tissue sections were cut and processed for tracer fluorescence microscopy and quantitative autoradiography, as previously described (30). In addition, samples of blood, plasma, and systemic tissues were collected for analysis by liquid scintillation counting or chromatography. Brain and brain metastasis lapatinib concentrations were corrected for residual intravascular drug by subtracting the product of vascular volume and terminal blood lapatinib concentration. For these corrections, vascular volumes of 0.01 ml/g and 0.007 ml/g were used for brain and brain metastasis, respectively (30).

Lapatinib Chromatographic Analysis

^{14}C-Lapatinib radiochemical integrity was determined prior to injection as well as in plasma and tissue samples obtained at the end of circulation using methods adapted from prior publications (20,21). Plasma samples (~100 μL) were treated with acetonitrile (4:1 v/v) and centrifuged to remove precipitant. Tissue samples (~0.1–0.2 g) were homogenized in water followed by precipitation with acetonitrile (4:1 v/v). Supernatants were evaporated to dryness and reconstituted with DMSO (10 μL) and mobile phase (100 μL). ^{14}C-Lapatinib reverse phase HPLC separation was performed using a Varian Prostar system (Model 410 autosampler with Model 230 solvent delivery module) linked to a C-18 Altima column (3 μm, 150× 4.6 mm). Mobile phase consisted of a mixture of 50 mM ammonium acetate buffer (pH-4.5) and acetonitrile with the percent acetonitrile increasing in a linear gradient over the course of the run. Flow rate was 1 mL/min. Solute detection was by UV spectrometry (Varian Prostar Model 325; λ=270 nm) for total lapatinib and flow scintillation analysis (Perkin Elmer AFSATR00 and Beckman 6500) for ^{14}C-lapatinib. Unlabeled lapatinib was analyzed by electrospray ionization LC-MS/MS (Varian 1200 L), as previously described (20,21).

Isolation of Lapatinib Resistant Cell Line

Mice that received intracardiac injections of 231-BR-HER2 brain metastases were assigned to receive either vehicle (0.5% hydroxypropylmethylcellulose with 0.1% Tween 80 in water), n=5 mice, or lapatinib (100 mg/kg body weight), n=10 mice twice daily by oral gavage for 24 days. Mice were euthanized by CO_2 asphyxiation at the end of treatment or when they showed signs of neurological impairment. The whole brain was removed from the skull, bisected along the sagittal plane and the left hemisphere was immediately frozen in Tissue-Tek OCT (Sakura Finetek USA, Torrance, CA). These samples were used for histology. The right hemisphere was isolated for tissue culture by cutting up the brain into small pieces into 10 cm plates in Dulbecco's modified Eagle Medium (DMEM, Invitrogen) supplemented with 10% fetal bovine serum (FBS, Invitrogen) plus 1% penicillin-streptomycin and 1% fungizone (amphotericin B). Tumor cells were grown out of 8 treated and 2 vehicle mouse brains. Each brain was cultured separately to establish independent cell lines.

Western Blot

Lapatinib-treated 231-BR-HER2 lines and 231-BR-HER2 non-treated lines were plated on 10 cm plates in DMEM plus 10% FBS plus 1% penicillin-streptomycin for 3 days.

At confluency, cells were harvested and lysed in RIPA buffer containing complete mini EDTA-free protease inhibitor cocktail (Roche). Total lysates were resolved by SDS-PAGE and transferred to nitrocellulose membranes. Immunoblot analysis was performed per standard procedures. Horseradish peroxidase-conjugated secondary antibodies were used at dilutions of 1:5000. Proteins were visualized using enhanced chemiluminescence (Cell Signaling Technology) and autoradiography.

Cell Viability Assay

231-BR-HER2 lapatinib-treated lines and 231-BR-HER2 non-treated lines were plated at a density of 2,000 cells/well in a 96-well plates in DMEM plus 10% FBS and incubated overnight to allow cells to adhere to the substratum. The cells were treated with various concentrations (4–10 μM) of lapatinib or with DMSO (i.e., the diluent for lapatinib) as a control. The number of viable cells was determined at 72 h after lapatinib addition by adding 3-(4,5-dimethyl-2-thiazolyl)-2,5-diphenyl-2H-tetrazolium bromide (MTT; Sigma) at a final concentration of 0.5 mg/mL to each well. After 2 h incubation at 37°C, DMSO was added to the well to solubilize the MTT, and absorbance measured at 570 nm. Data are shown as a percentage of the vehicle-treated line tested.

Lapatinib Resistant Cells *In Vitro*

231-BR-HER2 lapatinib-treated lines and 231-BR-HER2 non-treated lines were cultured in 1 μM lapatinib over 1 month period to achieve *in vitro* resistant cells.

Clonogenic Assay

231-BR-HER2 lapatinib-treated lines ($n=8$) and 231-BR-HER2 non-treated lines ($n=2$) were plated at a density of 200 cells/well in 6-well plates in DMEM plus 10% FBS and incubated overnight to allow cells to adhere to the substratum. The cells were treated with 4 μM lapatinib or DMSO. The cells were treated on day 1, 5, and 9 with day 0 being the plating day and stained on day 12. Cells were fixed in 80% methanol with 20% acetic acid for 1 h then stained with Wright Giemsa Stain (Eng Scientific, Inc).

Statistical Analysis

Data were analyzed for descriptive and inferential statistics using Prism 5 software (GraphPad). Results are presented as mean ± SD, unless otherwise noted. Statistical differences were assessed using nonparametric Mann Whitney or Kruskal Wallis tests. Pearson's correlation was used to calculate r^2 values. All tests were two-sided with $P<0.05$ for statistical significance.

RESULTS

Brain Distribution After Oral Dosing

^{14}C-Lapatinib (100 mg/kg) was administered orally to immunocompromised mice bearing 231-BR-HER2 metastases. Samples were collected at 2 or 12 h thereafter for determination of ^{14}C-lapatinib concentration in blood, plasma, and tissues. Sampling time points were chosen to correspond to blood C_{max} and C_{min} obtained with twice daily oral dosing of lapatinib (GSK unpublished data). The dose matched that previously used in the brain metastasis efficacy study of Gril *et al.* (28).

^{14}C-Lapatinib concentrations in brain at sites distant from metastases were low and uniform at both time points with mean values of 149 ng/g at 2 h and 55 ng/g at 12 h (Table I). Correction of brain for residual intravascular radioactivity, calculated as brain blood volume (1.0%) x terminal blood concentration (30), reduced mean brain lapatinib concentrations further to 97 and 49 ng/g, respectively. Lapatinib distribution to brain was low as these corrected values represented 1.3–2.8% of matching plasma concentrations (Table I). Calculated % dose to brain was 0.0025% of the administered oral dose. Tracer was confirmed as >92% intact in plasma and tissues by HPLC at 2 h after administration. The results are consistent with Polli *et al.* (20,21) showing restricted lapatinib distribution to brain in mice.

Brain Metastasis Distribution After Oral Dosing

In contrast to normal brain, experimental brain metastases exhibited variable and generally elevated ^{14}C- lapatinib concentrations which ranged from 100 to 2,890 ng/g at 2 h and from 8 to 1,300 ng/g at 12 h after oral dosing. Figure 1 presents representative images of ^{14}C-lapatinib distribution in brain metastases. In most cases, ^{14}C-lapatinib concentration significantly exceeded that in surrounding brain tissue ($P<0.05$). On average, brain metastasis lapatinib concentration was 7-fold greater than normal brain at 2 h and 9-fold greater at 12 h (Table I). By 12 h, the brain metastasis/plasma concentration ratio equaled 26%, indicating marked uptake over residual vascular drug (0.7%) (30).

Distribution analysis confirmed the heterogeneity of lapatinib concentration between brain metastases. As shown in Fig. 2a for 2 h animals, 70% of brain metastases showed moderately elevated ^{14}C-lapatinib with mean concentration of 528 ng/g and an average increase of 5-fold. In contrast, in 17.5% of brain metastases, ^{14}C-lapatinib was markedly elevated (mean concentration =1,698 ng/g; average elevation =18-fold) ($P<0.001$), whereas in 12.5% ^{14}C-lapatinib concentration did not differ significantly from normal brain. Comparable trends were noted in 12 h data (data not shown).

Table I Plasma, Blood, and Tissue ^{14}C-Lapatinib Concentrations at 2 and 12 h After Oral Administration of 100 mg/kg ^{14}C-Lapatinib

Sample	^{14}C-lapatinib concentration			
	2 h		12 h	
	(ng/g)	(μM)	(ng/g)	(μM)
Plasma	7,462 ± 910	7.91 ± 0.96	1,731 ± 381	1.84 ± 0.40
Blood	5,274 ± 527	5.59 ± 0.56	1,160 ± 255	1.23 ± 0.27
Brain	149 ± 52	0.16 ± 0.06	55 ± 29	0.06 ± 0.03
Brain (Vascular corrected)	97 ± 54	0.10 ± 0.06	49 ± 28	0.05 ± 0.03
Brain Metastasis (Vascular corrected)	672 ± 573	0.71 ± 0.61	454 ± 338	0.48 ± 0.36
Lung Metastasis	–	–	3,889 ± 360	4.12 ± 0.38
Heart Tumor	–	–	2,549 ± 689	2.70 ± 0.73

Values are mean ± SD for n-5-8 animals. Number of brain metastases equaled n = 160 and n = 46 at 2 and 12 h, respectively. The number of lung metastases equaled 9 whereas heart tumors equaled 3

Variability was also noted in ^{14}C-lapatinib concentration within brain metastases. As illustrated in Fig. 2b, ^{14}C-lapatinib concentrations ranged >100-fold between individual regions (25 × 25 μm) within individual brain metastases. No clear distinction was noted in lapatinib distribution between metastasis center or rim. In Fig. 2b, the mean ^{14}C- lapatinib concentration was 604 ng/g with individual regions varying from 30 to 4,300 ng/g. Lapatinib concentration fell off sharply at the edge of the brain metastases so that within 200–300 μm of the outer edge drug concentration approached normal brain values. Thus, though brain metastasis lapatinib concentrations are reported in this manuscript predominantly as mean values, this masks marked (>100-fold) intratumor and intertumoral variation.

Many brain metastases with elevated ^{14}C-lapatinib also showed increased BTB permeability to Texas Red 3 kDa dextran, as illustrated in Fig. 1. Because compromised BTB integrity may allow greater ^{14}C-lapatinib uptake, a correlation was performed between ^{14}C-lapatinib concentration and Texas Red dextran permeability for n=160 brain metastases. ^{14}C-Lapatinib was found to correlate significantly with BTB permeability (r^2=0.27, P<0.001) (Fig. 2c), consistent with a role of altered BTB integrity in enhanced lapatinib uptake. In contrast, only a weak correlation (r^2= 0.03) was found with metastasis size (mm^2)(Fig. 2d). A number of small micrometastases (<1 mm diameter) were found with markedly elevated lapatinib concentration (>10–20-fold). Similarly, a number of large metastases (>1–2 mm diameter) showed only limited lapatinib accumulation (<5–6-fold). Thus, the data differ from prior studies which suggested that BTB permeability may increase directly with tumor size (32,33). In our study, a small subset (<20%) of both small and large brain metastases exhibited marked (>10-fold) lapatinib accumulation which correlated with compromised BTB integrity.

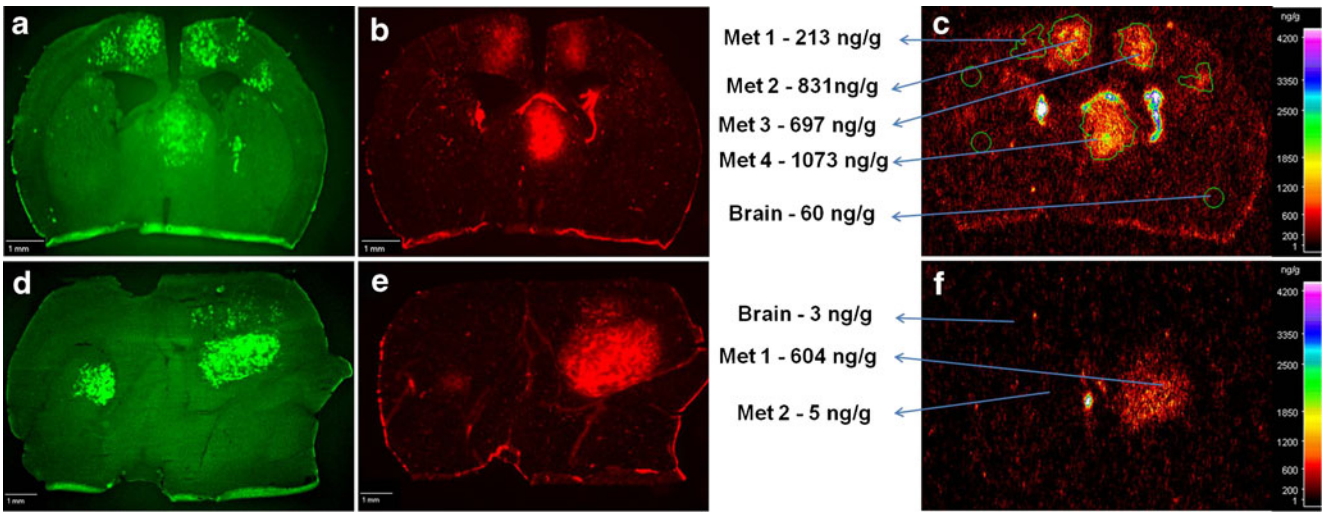

Fig. 1 ^{14}C-Lapatinib in brain and brain metastases at 2 (**a–c**) and 12 (**d–f**) hours following ^{14}C-lapatinib administration (100 mg/kg, p.o.) in mice with 231-BR-HER2 tumors**.** Representative coronal brain sections showing green EGFP metastasis fluorescence (**a,d**), Texas Red 3kD dextran fluorescence (**b,e**), and ^{14}C-lapatinib radioactivity (**c,f**) from an animal with 231-BR-HER2 brain metastases that received ^{14}C-lapatinib for 2 (**a–c**) or 12 (**d–f**) hours. Met = metastasis.

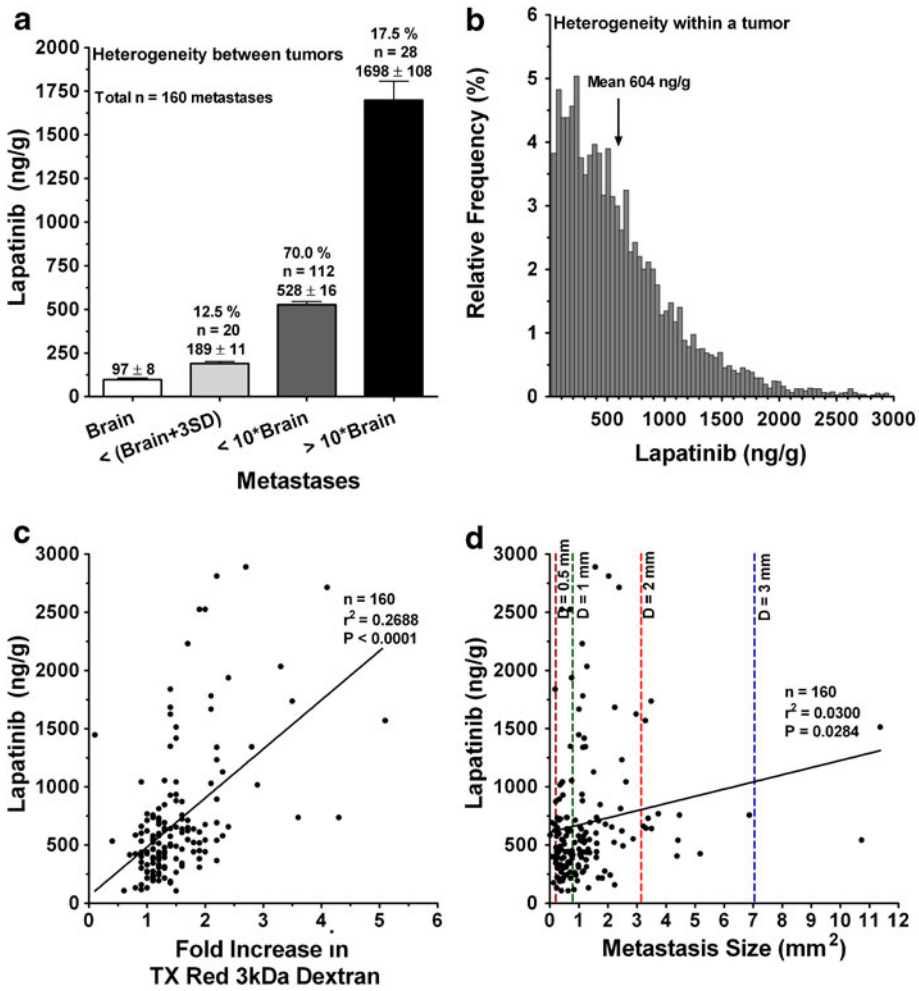

Fig. 2 Distribution of ^{14}C-lapatinib between (**a**) and within (**b**) brain metastases, as well as relation of ^{14}C-lapatinib concentration to metastasis size (**c**) and barrier permeability (**d**). Data are for animals ($n = 6$-8) at 2 h after oral administration of 100 mg/kg ^{14}C-lapatinib. Similar results were found at 12 h. (**a**) Brain metastasis ^{14}C-lapatinib concentrations were divided into three mutually exclusive groups: comparable to brain (<mean brain concentration + 3 x SD), <10-fold higher relative to brain, and >10-fold higher relative to brain. Bars represent group average concentration ± SEM. The percentage of metastases within each group is listed above the bar. (**b**) Distribution of ^{14}C-lapatinib concentration within a single representative brain metastasis (Met-1 in Fig. 1f). Each bar represents the relative frequency of concentration within small regions (pixel = 25 × 25 μm) of the tumor. Although the average concentration for the metastasis was 604 ng/g, individual regions within the metastasis varied from 30 to >4,300 ng/g. (**c,d**) Points represent data for individual brain metastases. Color dotted lines denote average metastasis diameter (D) in mm. The Pearson correlation is shown as a solid line and was statistically significant ($P < 0.05$).

Comparison with Peripheral Metastases

To further investigate the role of the BTB in limiting lapatinib distribution, ^{14}C-lapatinib concentrations were determined in systemic metastases and compared to those from the same animal in brain. The concept was that if one compared drug accumulation in two metastases from the same tumor cell line, one residing in the nervous system with a vascular barrier and one in systemic tissues without a vascular barrier, this may provide insight as to the function of the barrier system in limiting drug accumulation to CNS metastases. Twelve soft tissue metastases were found in peripheral tissues in the 12 h ^{14}C-lapatinib animals; most (75%) were in the lung. Figure 3 presents representative images from one animal with a lung metastasis. ^{14}C-Lapatinib concentrations were markedly greater in lung metastasis (3,464 ng/g) and surrounding normal lung tissue (20,784 ng/g) (Fig. 3) than those observed in matching brain metastases (454 ng/g). On average, brain metastasis ^{14}C-lapatinib concentration was only ~11% of that in lung metastases (Table I; Fig. 4). The ratio was even lower against many high uptake tissues, such as liver, kidney, and lung (Fig. 4). Only in a subset of brain metastases (17.5%) did lapatinib concentrations (~1,698 ng/g) approach those of peripheral metastases (2,549–3,889 ng/g) (Fig. 4). The markedly lower ^{14}C-lapatinib concentration in most brain metastases as compared to matching metastases in systemic tissues provides additional support for the hypothesis that the BTB plays a significant role in limiting lapatinib distribution to metastases in the CNS.

Verification with Intravenous Dosing

Although >92% of the ^{14}C-lapatinib tracer was intact at 2 h after oral administration, it is possible that small levels of tracer metabolites or breakdown products impact the findings of the oral dosing experiments. Therefore, to confirm the finding that brain metastasis ^{14}C-lapatinib uptake was limited, matching experiments were performed in animals with short term (30 min) *i.v.* ^{14}C-lapatinib (10 mg/kg) dosing. Under these conditions, >98% of the plasma ^{14}C tracer was confirmed as intact ^{14}C-lapatinib (Fig. 5). Similar to oral dosing, *i.v.* ^{14}C-lapatinib adminis-

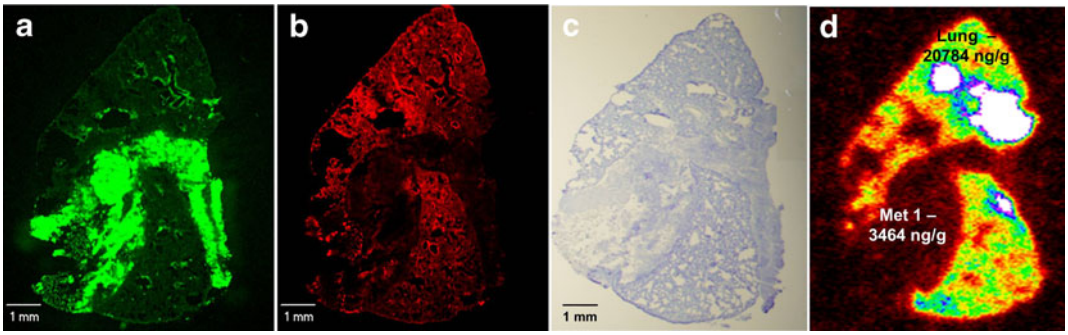

Fig. 3 ^{14}C-Lapatinib in lung (**a–d**) metastases at 12 h after ^{14}C-lapatinib administration (100 mg/kg, oral)**.** Representative sections showing lung metastasis EGFP fluorescence (**a**), Texas Red 3 kDa dextran fluorescence (**b**), cresyl violet staining (**c**) and ^{14}C-autoradiography (**d**) from an animal with 231-BR-HER2 metastases that received ^{14}C-lapatinib at 12 h prior to euthanasia. Matching metastases were also measured in brain from the same animal.

tration was associated with significantly elevated ^{14}C-lapatinib radioactivity in most brain metastases relative to surrounding brain (Fig. 6). The average fold lapatinib accumulation in brain metastases (3.2-fold) relative to normal brain was somewhat less than that with oral dosing and longer circulation times. However, the mean brain metastasis lapatinib concentration (412 ng/g) and the peak values (1,000–3,000 ng/g) were similar to those seen with oral dosing, verifying the heterogeneity and general effect. As was observed with oral administration, brain metastasis ^{14}C-lapatinib uptake after *i.v.* administration correlated significantly with BTB permeability ($P=0.0004$, $n=77$), Average ^{14}C-lapatinib concentrations in brain metastases were 1–2 orders of magnitude less than those in peripheral tissues (Fig. 6). No soft tissue peripheral metastases were found in animals used in the *i.v.* administration experiments. The results support the conclusion that the BTB plays a role in limiting lapatinib distribution to brain metastases and that the results were not artifacts of tracer breakdown or metabolism.

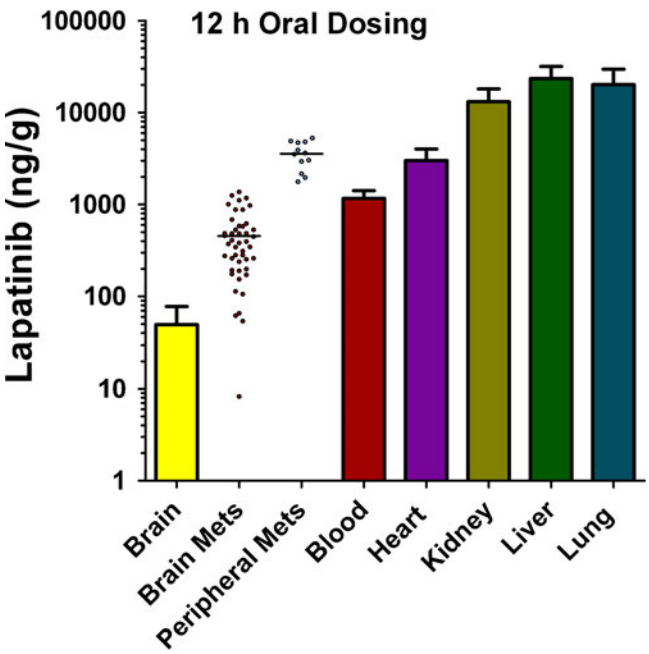

Fig. 4 ^{14}C-Lapatinib concentrations in brain and peripheral metastases, as well as blood and other tissues, at 12 h after ^{14}C-lapatinib administration (100 mg/kg, oral) in immunocompromised mice with 231-BR-HER2 metastases**.** Bars represent mean ± SD for $n=5$ animals. Lapatinib concentration (y-axis) is shown in log scale. Points represent concentrations in individual metastases; mean concentration is shown by a line.

Generation and Characterization of Resistant Cell Lines from Brains of Lapatinib-Treated Mice

To evaluate whether drug resistance played a role in limited lapatinib efficacy against brain metastases, 231-BR-HER2 cells were injected into the left cardiac ventricle of immunocompromised mice and animals were administered lapatinib (100 mg/kg *p.o.*) twice daily for 24 days. At necropsy one hemisphere of the brain was placed in growth media and dissected under sterile conditions to isolate tumor cells for culture. Eight lapatinib-treated and two vehicle-treated cultures were established. A western blot of cell lysates from these cultures indicated that HER2 expression was maintained throughout *in vivo* treatment and *ex vivo* culture (Fig. 7). To determine if the cell lines established from lapatinib-treated brains were resistant to lapatinib, cells were tested for responsiveness to lapatinib *in vitro* in viability and clonogenic assays. Cells were treated with 8 or 10 μM lapatinib for 72 h, and viability measured by MTT assay (Fig. 8a,b). All cell lines were sensitive to lapatinib inhibition, and no differences were observed between the lapatinib *versus* vehicle treatment ($P>0.05$). It remained possible that the short culture period in normal tissue culture conditions reversed *in vivo* lapatinib resistant phenotypes, therefore frozen stocks of *ex vivo* cultures were expanded in 1 μM lapatinib for 1 month. When tested in viability assays, equivalent results were obtained (data not shown). Finally, clonogenic assays demonstrated an inhibitory effect of lapatinib that was comparable between lapatinib- and vehicle-treated cultures (Fig. 8c). The data indicate that tumor cells remaining in the brain after lapatinib treatment were sensitive to lapatinib *in vitro*.

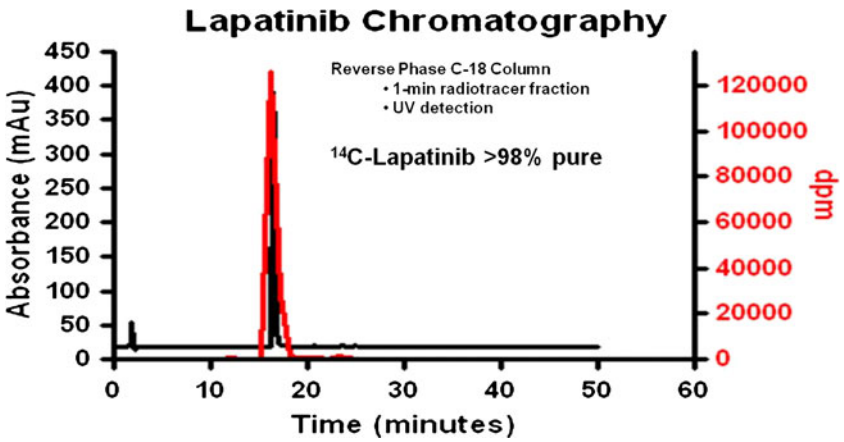

Fig. 5 Radiochromatography of ^{14}C-radioactivity in plasma at 30 min after intravenous administration of 10 mg/kg ^{14}C-lapatinib**.** Radiolabeled lapatinib was found to be >98% pure and co-eluted with cold lapatinib as confirmed with HPLC.

DISCUSSION

The therapy of brain metastases represents a significant unmet medical need. Standard chemotherapy with agents such as paclitaxel and doxorubicin is associated with very limited or no short-term positive effect on brain metastases (34). Trastuzumab, an anti-HER2 antibody, has significant positive therapeutic action on HER2+ systemic breast tumors, but shows minimal transport across the BBB (12,14,15,35). The results of this study demonstrate that ^{14}C-lapatinib delivery is elevated in a great majority (>85%) of brain metastases of breast cancer using the human 231-BR-HER2 breast cancer model in immunocompromised mice. On average, lapatinib concentrations in brain metastases are elevated 7–9-fold over those in surrounding brain tissue. However, brain metastasis lapatinib distribution is highly heterogeneous, and in the majority of brain metastases lapatinib concentrations are still only a fraction (<10–20%) of those in peripheral metastases. Only in a subset of cases (17%) did brain metastasis lapatinib concentrations approach those of peripheral tumors. For optimal therapy, good lapatinib distribution would be desirable in all or most all brain metastases, comparable to systemic metastases. A strong correlation was noted between brain metastasis lapatinib concentration and BTB permeability. The results demonstrate that lapatinib distribution to brain metastases of breast cancer is restricted and varies with BTB permeability which differs within and between tumors. The results support the hypothesis that lapatinib efficacy is limited in brain metastases by restricted drug delivery.

Of all the tissues studied, the brain showed the lowest lapatinib distribution. Measured brain-to-plasma concentration ratios for lapatinib after vascular correction equaled 0.013 and 0.028 in this study. Similar values were obtained by Polli *et al.* (20,21) following *i.v.* lapatinib infusion to steady state (24 h) in mice, with total brain/plasma lapatinib ratios of 0.03–0.04 at comparable plasma con-

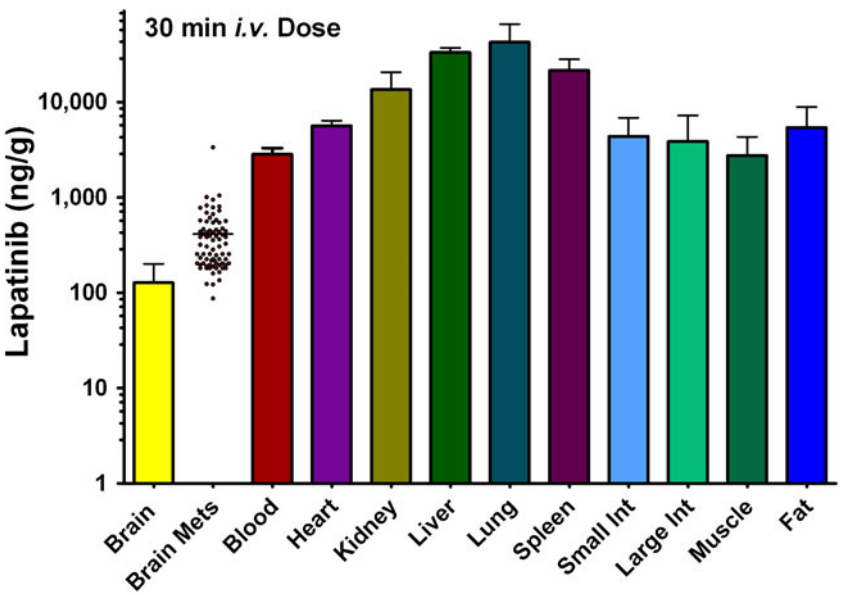

Fig. 6 ^{14}C-Lapatinib distribution at 30 min after *i.v* ^{14}C-lapatinib administration (10 mg/kg) in immunocompromised mice with 231-BR-HER2 metastases**.** Bars represent mean ± SD for $n = 3$ animals. Lapatinib concentration (y-axis) is shown in log scale. Points represent concentrations in individual metastases; mean concentration is shown by a line.

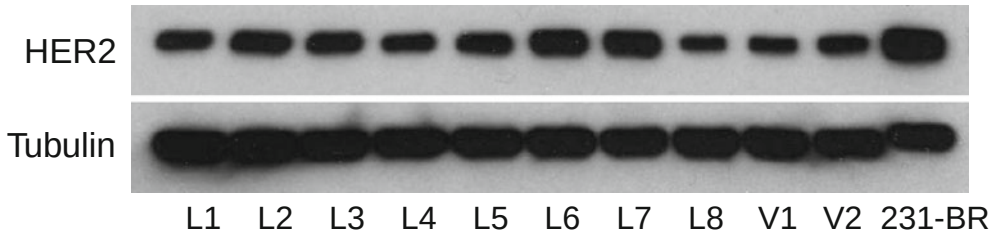

Fig. 7 HER2 expression is maintained upon *ex vivo* culture of lapatinib-treated brain metastatic tumor cells. 231-BR-HER2 cells were injected into immunocompromised mice, treated with either 100 mg/kg lapatinib twice daily or vehicle. At necropsy, tumor cells were cultured *ex vivo* from brains of lapatinib-treated (L) or vehicle-treated (V) mice. The HER2 expression of lysates of each culture was determined by western blot, using α-tubulin as a loading control.

centrations (730 and 5,097 ng/g). Vascular correction would lower their values by ~0.01 mL/g, providing ratios (0.02–0.03) which match well to ours and indicate only very limited brain lapatinib accumulation. The low distribution of lapatinib to brain has been linked to active lapatinib efflux transport at the BBB by P-gp (ABCB1) and BCRP (ABCG2) (20,21). Steady-state brain-to-plasma distribution ratios for lapatinib were 4-5-fold higher (0.08–0.15) in P-gp knockout mice. However, knockout of both P-gp and BCRP increased brain-to-plasma lapatinib ratio by >50–60-fold to 1.2–1.7 (21), indicating that both transporters contribute to limiting lapatinib distribution to brain. Multiplying the vascularly-corrected brain concentrations in our study by 60-fold places them in the range of systemic tissues without a BBB. For example, in the 12 h oral dose lapatinib experiments, 60 times the brain lapatinib concentration of 49 ng/g equals 2,940 ng/g, which is comparable to that measured in peripheral metastases (2,000–4,000 ng/g) at the same time point. The results support the notion that BBB limits lapatinib distribution to brain and suggest the overall deficit in delivery may be >50–60-fold based upon efflux transport. Plasma lapatinib concentration declined 4-fold between 2 and 12 h after oral administration, consistent with the reported plasma half-life of 4–6 h in mice (21). In most tissues, marked lapatinib sequestration was evident in tissues, consistent with the large volume of distribution for lapatinib of 9.5 L/kg (36).

In brain metastases of the 231-BR-HER2 breast cancer model, lapatinib distribution increased on average by 7–9-fold over surrounding normal brain, attaining mean brain-to-plasma ratios of 0.09 at 2 h and 0.26 at 12 h. Yet, average brain metastasis lapatinib concentrations were still 6–10-fold less than matching concentration in peripheral metastases, suggesting that barrier compromise was only partial and that significant restriction still remained to lapatinib accumulation. Enhanced brain metastasis drug uptake may arise from increased BTB passive permeability or decreased expression and function of BTB active efflux transporters (22,37). The Texas Red 3 kDa dextran results show clear enhanced BTB passive permeability in most brain metastases which correlated with lapatinib uptake. The expression and function of active efflux transporters at the BTB has not been clearly defined. Our preliminary P-gp staining data with the brain 231-BR-HER2 model, suggest that BTB P-gp is maintained in many brain lesions (30). This is supported by *in vivo* and brain perfusion results showing >40-fold enhancement in brain metastasis uptake of paclitaxel in the same metastasis model in the presence of active efflux transport inhibitors, such as tariquidar and elacridar (Taskar *et al.* Role of blood–brain barrier transporters in the brain uptake of the anticancer drug, paclitaxel; Abstract # T3435 presented at AAPS Annual Meeting and Exposition, New Orleans, LA, November 2010). Expression and function of active efflux transporters by tumor cells within the brain may also play a role in limiting accumulation. Additional work is required to define the specific BTB mechanisms that drive variably enhanced lapatinib uptake in brain metastases. The marked heterogeneity in brain metastasis lapatinib uptake, which correlates within and between lesions with BTB passive integrity, suggests that barrier alteration plays a critical role.

In this study, only 17% of brain metastases showed marked lapatinib accumulation which fell within 2–4-fold of that in peripheral metastases. In the great majority of brain metastases, lapatinib distribution was far lower and highly variable. These findings are consistent with clinical and preclinical studies showing only partial efficacy of lapatinib against HER2+ brain metastases of breast cancer. For example, Gril *et al.*, using the same lapatinib dose and tumor model, found a ~50% reduction in the number of large brain metastases and no change in the number of micrometastases (28). In our study at the same dose, the total lapatinib concentration attained in highest brain metastases (>2,000 ng/g at 2 h and >1,000 ng/g at 12 h; ~1–3 μM) exceeds the reported K_D of lapatinib binding to HER2 (13 nM) (19) but is still less than the IC_{50} for inhibition of 231-BR-HER2 proliferation *in vitro* (8 μM)(28). Lapatinib activity *in vivo* may benefit from the slow disassociation halftime of the drug from the HER2 receptor ($t_{1/2}$=6 h) as well as the prolonged time it takes HER2 to recover from inhibition of receptor phosphorylation (e.g., 15% recovery in 4 days) (19). So, the potential exists for

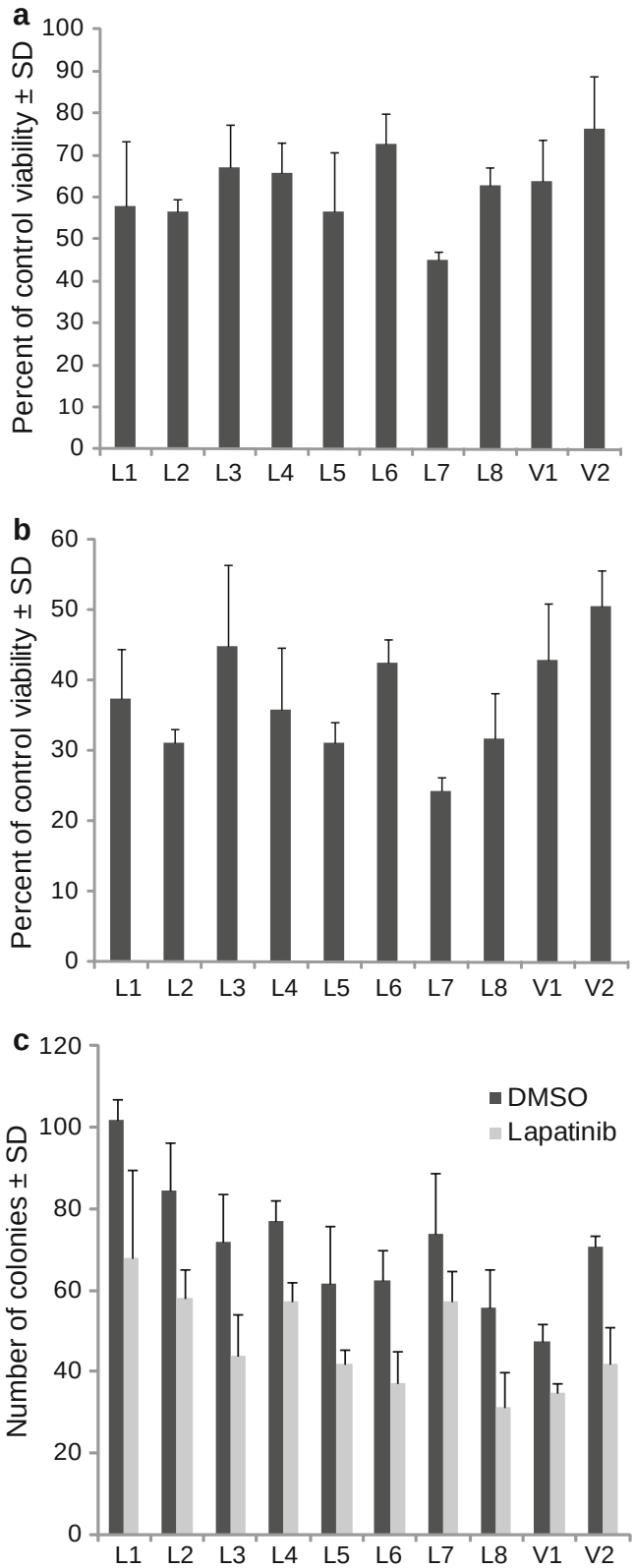

Fig. 8 *Ex vivo* cultures of lapatinib-treated 231-BR-HER2 cells remain sensitive to lapatinib *in vitro*. (**a–b**) Cultures described in Fig. 7 were assayed for viability after 72 h of lapatinib treatment (8 μM lapatinib, **a**; 10 μM lapatinib, **b**) by MTT assay. Data represent the mean ± SD of triplicate cultures. (**c**) Clonogenic assays of the *ex vivo* cultures in 4 μM lapatinib.

cumulative effects. However, with heterogeneous lapatinib distribution, the majority of brain metastases are exposed to significantly lower drug levels, and in 12.5% of metastases, drug exposure did not differ significantly from surrounding brain tissue. At 2 h after oral administration, the lapatinib concentration in normal brain and in 70% of brain metastases showing only limited elevation was in the range of 100–500 ng/g or ~100–500 nM. Assuming a lapatinib free fraction of 1% in brain based upon the cLogP of 5.1 (38,39), this predicts that free lapatinib concentrations in brain and a significant fraction of brain metastases are on the order of $0.01 \times 100–500 = 1–5$ nM, which is three order of magnitude less than the concentration which inhibits cell proliferation *in vitro* and less than the K_D of the HER2 receptor. In contrast, the predicted free lapatinib in the highest brain metastases ($0.01 \times 3{,}000 = 30$ nM) would significantly exceed the K_D of the HER2 and be suggestive of activity. Thus, the results suggest that while lapatinib reaches active concentrations in some brain metastases, restricted and heterogeneous delivery in others will limit the efficacy of the drug in the treatment of brain metastases of breast cancer.

Drug resistance has also been suggested as a possible mechanism to explain only partial lapatinib activity against brain metastases of HER2+ breast cancer (25). Most studies of lapatinib resistance to date have been exclusively *in vitro*, using long term culture of tumor cell lines exposed to drug. From these studies, multiple potential avenues of resistance have emerged including PI3K/PTEN/Akt (40,41), hormone receptor signaling (42), Erk (41), HER2 mutation (42) and the Axl pathway (43). To test whether drug resistance was a factor in our study, eight cell lines were established from brains of mice injected with 231-BR-HER2 cells and treated at the same dose with lapatinib for 24 days. As compared to two cell lines established from vehicle-treated mice, the *in vitro* lapatinib responsiveness of these cultures was comparable. No differences in viability by MTT assay or colony formation by clonogenic assay were observed. The results suggest that the tumor cells in brain metastases remain lapatinib sensitive and that drug resistance was not a factor. It is possible that resistance pathways emerged *in vivo* but were lost upon short-term *ex vivo* culture.

Overall, the findings support the hypothesis that restricted lapatinib delivery contributes to partial lapatinib efficacy against HER2+ brain metastases of breast cancer. The BTB, though compromised in integrity, still limits brain lapatinib exposure in many brain metastases to <10–20% of those in systemic metastases and with marked variability within and between lesions. The data suggest that compounds with improved BBB permeability and synergy with lapatinib would be helpful for HER2+ brain metastatic breast cancer. Brain metastasis delivery may be enhanced by drugs that modify the barrier to either down regulate

efflux transporter function, increase BBB passive permeability, or shuttle lapatinib into brain by carrier- or receptor-mediated mechanisms.

ACKNOWLEDGMENTS & DISCLOSURES

Drs. Rubin, Castellino, and Polli work for GlaxoSmithKline, which owns the patent to lapatinib, and thus have a financial interest.

Grant Support Intramural Program of the National Cancer Institute (P.S.S., D.P.), grant W81XWH-062-0033 from the Department of Defense Breast Cancer Research Program (P.S.S., Q.R.S., P.R.L., and D.P.), grants R01 NS052484 and R01 NS052484-04S1 from NINDS/NIH (Q.R.S.) and GlaxoSmithKline grant to Q.R.S.

REFERENCES

1. Hynesand NE, Lane HA. ERBB receptors and cancer: the complexity of targeted inhibitors. Nat Rev Cancer. 2005;5:341–54.
2. Lin N, Bellon J, Winer E. CNS metastases in breast cancer. J Clin Oncol. 2004;22:3608–17.
3. Leyland-Jones B. Human epidermal growth factor receptor 2-positive breast cancer and central nervous system metastases. J Clin Oncol. 2009;27:5278–86.
4. Clayton AJ, Danson S, Jolly S, Ryder WD, Burt PA, Stewart AL, *et al.* Incidence of cerebral metastases in patients treated with trastuzumab for metastatic breast cancer. Br J Cancer. 2004;91:639–43.
5. Bendell JC, Domchek SM, Burstein HJ, Harris L, Younger J, Kuter I, *et al.* Central nervous system metastases in women who receive trastuzumab-based therapy for metastatic breast carcinoma. Cancer. 2003;97:2972–7.
6. Slamon DJ, Leyland-Jones B, Shak S, Fuchs H, Paton V, Bajamonde A, *et al.* Use of chemotherapy plus a monoclonal antibody against HER2 for metastatic breast cancer that overexpresses HER2. N Engl J Med. 2001;344:783–92.
7. Piccart-Gebhart MJ, Procter M, Leyland-Jones B, Goldhirsch A, Untch M, Smith I, *et al.* Trastuzumab after adjuvant chemotherapy in HER2-positive breast cancer. N Engl J Med. 2005;353:1659–72.
8. Romond EH, Perez EA, Bryant J, Suman VJ, Geyer Jr CE, Davidson NE, *et al.* Trastuzumab plus adjuvant chemotherapy for operable HER2-positive breast cancer. N Engl J Med. 2005;353:1673–84.
9. Musolino A, Ciccolallo L, Panebianco M, Fontana E, Zanoni D, Bozzetti C, *et al.* Multifactorial central nervous system recurrence susceptibility in patients with HER2-positive breast cancer: epidemiological and clinical data from a population-based cancer registry study. Cancer 2010.
10. Bria E, Cuppone F, Fornier M, Nistico C, Carlini P, Milella M, *et al.* Cardiotoxicity and incidence of brain metastases after adjuvant trastuzumab for early breast cancer: the dark side of the moon? A meta-analysis of the randomized trials. Breast Cancer Res Treat. 2008;109:231–9.
11. Lin NU, Winer EP. Brain metastases: the HER2 paradigm. Clin Cancer Res. 2007;13:1648–55.
12. Pestalozziand BC, Brignoli S. Trastuzumab in CSF. J Clin Oncol. 2000;18:2349–51.
13. Lampson LA. Monoclonal antibodies in neuro-oncology: getting past the blood-brain barrier. MAbs. 2011;3:153–60.
14. Stemmler HJ, Schmitt M, Willems A, Bernhard H, Harbeck N, Heinemann V. Ratio of trastuzumab levels in serum and cerebrospinal fluid is altered in HER2-positive breast cancer patients with brain metastases and impairment of blood-brain barrier. Anticancer Drugs. 2007;18:23–8.
15. Dijkers EC, Oude Munnink TH, Kosterink JG, Brouwers AH, Jager PL, de Jong JR, *et al.* Biodistribution of 89Zr-trastuzumab and PET imaging of HER2-positive lesions in patients with metastatic breast cancer. Clin Pharmacol Ther. 2010;87:586–92.
16. Kinoshita M, McDannold N, Jolesz FA, Hynynen K. Noninvasive localized delivery of Herceptin to the mouse brain by MRI-guided focused ultrasound-induced blood-brain barrier disruption. Proc Natl Acad Sci USA. 2006;103:11719–23.
17. Ryan Q, Ibrahim A, Cohen M, Johnson J, Ko C-W, Sridhara R, *et al.* FDA drug approval summary: Lapatinib in combination with capecitabine for previously treated metastatic breast cancer that overexpresses HER-2. The Oncologist. 2008;13:1114–9.
18. Rusnak DW, Affleck K, Cockerill SG, Stubberfield C, Harris R, Page M, *et al.* The characterization of novel, dual ErbB-2/EGFR, tyrosine kinase inhibitors: potential therapy for cancer. Cancer Res. 2001;61:7196–203.
19. Wood ER, Truesdale AT, McDonald OB, Yuan D, Hassell A, Dickerson SH, *et al.* A unique structure for epidermal growth factor receptor bound to GW572016 (Lapatinib): relationships among protein conformation, inhibitor off-rate, and receptor activity in tumor cells. Cancer Res. 2004;64:6652–9.
20. Polli JW, Humphreys JE, Harmon KA, Castellino S, O'Mara MJ, Olson KL, *et al.* The role of efflux and uptake transporters in [N-{3-chloro-4-[(3-fluorobenzyl)oxy]phenyl}-6-[5-({[2-(methylsulfonyl) ethy l]amino}methyl)-2-furyl]-4-quinazolinamine (GW572016, lapatinib) disposition and drug interactions. Drug Metab Dispos. 2008;36:695–701.
21. Polli JW, Olson KL, Chism JP, John-Williams LS, Yeager RL, Woodard SM, *et al.* An unexpected synergist role of P-glycoprotein and breast cancer resistance protein on the central nervous system penetration of the tyrosine kinase inhibitor lapatinib (N-{3-chloro-4-[(3-fluorobenzyl)oxy]phenyl}-6-[5-({[2-(methylsulfonyl)ethy l]amino}methyl)-2-furyl]-4-quinazolinamine; GW572016). Drug Metab Dispos. 2009;37:439–42.
22. Gerstner E, Fine R. Increased permeability of the blood-brain barrier to chemotherapy in metastatic brain tumors: Establishing a treatment paradigm. J Clin Oncol. 2007;25:2306–12.
23. Steeg PS, Camphausen KA, Smith QR. Brain metastases as preventive and therapeutic targets. Nat Rev Cancer. 2011;11:352–63.
24. Lin N, Carey L, Liu M, Younger J, Come S, Ewend M, *et al.* Phase II trial of lapatinib for brain metasetases in patients with human epidermal growth factor receptor 2-positive breast cancer. Clin Cancer Res. 2008;26:1993–9.
25. Lin N, Dieras V, Paul D, Lossignol D, Christodoulou C, Stemmler H-J, *et al.* Multicenter Phase II study of lapatinib in patients with brain metastases from HER-2 positive breast cancer. Clin Cancer Res. 2009;15:1452–9.
26. Sutherland S, Ashley S, Miles D, Chan S, Wardley A, Davidson N, *et al.* Treatment of HER2-positive metastatic breast cancer with lapatinib and capecitabine in the lapatinib expanded access programme, including efficacy in brain metastases–the UK experience. Br J Cancer. 2010;102:995–1002.
27. Metro G, Foglietta J, Russillo M, Stocchi L, Vidiri A, Giannarelli D, *et al.* Clinical outcome of patients with brain metastases from HER2-positive breast cancer treated with lapatinib and capecitabine. Ann Oncol. 2011;22:625–30.
28. Gril B, Palmieri D, Bronder JL, Herring JM, Vega-Valle E, Feigenbaum L, *et al.* Effect of lapatinib on the outgrowth of metastatic breast cancer cells to the brain. J Natl Cancer Inst. 2008;100:1092–103.

29. Cameron D, Casey M, Press M, Lindquist D, Pienkowski T, Romieu CG, *et al.* A phase III randomized comparison of lapatinib plus capecitabine *versus* capecitabine alone in women with advanced breast cancer that has progressed on trastuzumab: updated efficacy and biomarker analyses. Breast Cancer Res Treat. 2008;112:533–43.
30. Lockman PR, Mittapalli RK, Taskar KS, Rudraraju V, Gril B, Bohn KA, *et al.* Heterogeneous blood-tumor barrier permeability determines drug efficacy in experimental brain metastases of breast cancer. Clin Cancer Res. 2010;16:5664–78.
31. Palmieri D, Bronder JL, Herring JM, Yoneda T, Weil RJ, Stark AM, *et al.* Her-2 overexpression increases the metastatic outgrowth of breast cancer cells in the brain. Cancer Res. 2007;67:4190–8.
32. Hasegawa H, Ushio Y, Hayakawa T, Yamada K, Mogami H. Changes of the blood-brain barrier in experimental metastatic brain tumors. J Neurosurg. 1983;59:304–10.
33. Fidler IJ. The role of the organ microenvironment in brain metastasis. Semin Cancer Biol. 2011;21:107–12.
34. Walbertand T, Gilbert MR. The role of chemotherapy in the treatment of patients with brain metastases from solid tumors. Int J Clin Oncol. 2009;14:299–306.
35. Pestalozzi BC. Correction: Meningeal carcinomatosis from breast carcinoma responsive to trastuzumab. J Clin Oncol. 2001;19: 4091.
36. Scheffler M, Di Gion P, Doroshyenko O, Wolf J, Fuhr U. Clinical pharmacokinetics of tyrosine kinase inhibitors: focus on 4-anilinoquinazolines. Clin Pharmacokinet. 2011;50:371–403.
37. Deeken JF, Loscher W. The blood-brain barrier and cancer: transporters, treatment, and Trojan horses. Clin Cancer Res. 2007;13:1663–74.
38. Summerfield SG, Read K, Begley DJ, Obradovic T, Hidalgo IJ, Coggon S, *et al.* Central nervous system drug disposition: the relationship between *in situ* brain permeability and brain free fraction. J Pharmacol Exp Ther. 2007;322:205–13.
39. Wan H, Rehngren M, Giordanetto F, Bergstrom F, Tunek A. High-throughput screening of drug-brain tissue binding and in silico prediction for assessment of central nervous system drug delivery. J Med Chem. 2007;50:4606–15.
40. Eichorn P, Gili M, Scaltriti M, Serra V, Guzman M, Nijkamp W, *et al.* Phosphatidylinositol 3-kinase hyperactivation results in lapatinib resistance that is reversed by the mTOR/phosphatidylinositol 3-kinase inhibitor NVP-BEZ235. Cancer Res. 2008;68:9221–30.
41. Zhou H, Kim Y-S, Peletier A, McCall W, Earp H, Sartor C. Effects of the EGFR/HER2 kinase inhibitor GW572016 on EGFR- and HER2-overexpressing breast cancer cell line proliferation, radiosensitization and resistance. Int J Rad Oncol Biol Physics. 2004;58:344–52.
42. Wang S, Narasanna A, Perez-Torres M, Xiang B, Wu F, Yang S, *et al.* HER2 kinase domain mutation results in constitutive phosphorylation and activation of HER2 and EGFR and resistance to EGFR tyrosine kinase inhibitors. Cancer Cell. 2006;10:25–38.
43. Liu L, Greger J, Shi H, Liu Y, Greshock J, Annan R, *et al.* Novel mechanism of lapatinib resistance in HER2-positive breast tumor cells: Activation of AXL. Cancer Res. 2009;69:6871–8.